CONF-970465--10 SAN096-2339C
SAND--96-2339C

Case Study: Unattended Ground Sensor Phenomenology and Signal Processing

Ireena A. Erteza[a], Greg. J. Elbring[a], Tim S. McDonald[a], John P. Claassen[a]
Doug R. Baumgardt,[b]
Jim K. Wolford[c]

[a]Sandia National Labs, MS 0843; Albuquerque, NM 87185-0843
[b]ENSCO Inc., 5400 Port Royal Road, Springfield, VA 22151
[c]Lawrence Livermore National Labs; L-183, PO Box 808, Livermore, CA 94551

ABSTRACT

In the fall of 1995, a unique unattended ground sensor experiment was conducted at the Nevada Test Site. In the experiment, a variety of electro-mechanical equipment was operated, while data was gathered using a number of different types of unattended sensors at different locations. The sensors in this study included seismometers, accelerometers, electric dipole sensors, magnetometers and microphones. In this paper, we present some key results from the signal processing of the data from this experiment.
The goal of the signal processing was to quantify some of the effects of range on signal propagation, and to determine the ability to detect signals from the equipment, to identify the equipment and to locate the equipment. Some of the physical phenomenon which can affect unattended ground sensor performance will be discussed. The paper will also include a discussion of how the geophysical site characteristics can affect the performance of unattended ground-deployed sensors.

Key Words: sensors, seismology, signal processing, signal propagation, unattended ground sensors

The field of unattended ground sensor systems is growing, and there are many potential uses and benefits for these systems. As with any sensor system, the data from unattended ground sensors must be gathered and processed, and some useful information must result from that processing. There are many factors which can affect the performance of the signal processing algorithms used to obtain information from unattended ground sensors. In this paper, we will explore a few physical phenomenon which can affect unattended ground sensor system performance.

In the fall of 1995, a unique unattended ground sensor experiment was conducted at the Nevada Test Site. In the experiment, a variety of electro-mechanical equipment was operated, while data were gathered using a number of different types of unattended sensors at different locations. This is illustrated in Figure 1. The sensors in this study included seismometers, accelerometers, electric dipole sensors, magnetometers and microphones. The purpose of this experiment was to gather data to explore and understand the performance of unattended ground sensor systems and the physical phenomenon that can affect them. While data from a number of different types of sensors were gathered in this experiment, in this paper we will concentrate on physical phenomenon which can affect seismic sensors and the processing of seismic data. The seismic sensors used in the experiment were geophones and accelerometers. The quantities measured are particle velocity and particle acceleration, respectively. The results presented here are from geophone data.

Before going on, it is helpful to briefly cover some pertinent information regarding seismic wave propagation. In general, seismic energy from a source transmits outwardly from the source in the from of seismic waves. Seismic waves follow the classic equations associated with wave propagation:

$$\frac{\partial^2 y}{\partial t^2} = c^2 \nabla^2 y$$

Sandia is a multiprogram laboratory operated by Sandia Corporation, a Lockheed Martin Company, for the United States Department of Energy under contract DE-AC04-94AL85000.

DISCLAIMER

$$\nabla^2 = \frac{\partial^2}{\partial x_i}$$

Depending on qualities of the medium of propagation and boundary conditions, a variety of solutions exist for the wave equation. These include body waves (longitudinal compression (P) and transverse shear (S) waves) and surface waves (Rayleigh waves and Love waves). There are unique velocities and particle motions associated with these different wave solutions.

Seismic waves have the same type of behavior normally associated with other types of wave propagation. There is a falloff of energy with distance (due to geometric spreading of the wave and also due to absorption via the frictional dissipation of energy into heat). In addition, seismic waves will reflect, refract and diffract. The reflection and refraction are often visualized using ray theory. In general, when any compressional wave is obliquely incident on an interface between two different media, it will be transformed into 4 kinds of waves: a reflected compressional, a reflected shear, a refracted shear and refracted compressional. This is illustrated in Figure 2.

The purposes of unattended ground sensor systems vary greatly. In general, however, the performance of a system (i.e. the ability to obtain the desired results from the data) depends on certain factors. These include the number, location and type of sensor used, the algorithmic complexity of the signal processing technique used, the signal to noise ratio of the data and the characteristics of the modes in which energy is propagated from source to sensor.

Critical to all algorithm performance is the signal to noise ratio. Unattended ground sensors are generally separated from the sources by some distance, and it is of interest to know how the signal to noise ratio (SNR) varies as a function of distance. Figure 3 is a plot of SNR vs. Frequency as a function of source-sensor separation. The sensor in this case is a 10Hz geophone. As one would expect for a homogenous medium, the analysis shows that all frequencies attenuate with distance, but the higher frequencies attenuate more quickly. The peaks at the higher frequencies are attributed to the sensor's sensitivity (response) with frequency.

The amplitude of any seismic wave is dependent on numerous factors including source coupling, receiver coupling, source-receiver distance and the properties of the material through which the seismic wave propagates. The last factor is what is most interesting as a geophysical characteristic. If an estimate of the attenuation characteristics of the material at a site can be made, then this value can be compared to the attenuation characteristics for other geologies of interest, and the effect of any differences on the function of the sensor system can be predicted.

In general, the amplitude of any seismic wave propagating through an attenuative medium can be expressed by:

$$A(R,\omega) = (1/R)A_0(R_0,\omega)\exp(-\alpha R)\exp(-i\omega R/v)$$

where A is the amplitude, R is the travel path length, ω is the angular frequency, α is the attenuation coefficient, and v is the wave velocity (Badri and Mooney, 1987)[1]. For seismic studies, attenuation is usually expressed as a Q value, which is defined as the ratio of 2π times the peak energy in a cycle to the energy dissipated. This can be expressed in terms of the attenuation coefficient as $Q = \omega / 2v\alpha$. The Q value is dependent on numerous properties of the rock including composition, porosity, confining pressure, fluid saturation, and degree of consolidation. As Q increases, the attenuation rate of the seismic energy decreases and measurable signal levels can be recorded at greater distances under the same background conditions.

In field measurements, the Q value can be determined using the spectral ratio technique in either the time domain or frequency domain (Badri and Mooney, 1987[1]; Vassiliou et al., 1984[5]). For our experiment site, data from an explosive-source refraction line collected 300 m east of the center were used. Peak-to-peak amplitudes of the first-arriving P-wave energy were measured for a variety of receiver pairs with a range in both distance of separation between the receivers and distance from the source to the near receiver of the pair. Q can be determined from the ratio of these amplitudes for any receiver pair using the following relationship:

$$1/Q = \frac{2}{\omega(T_2 - T_1)}\left[-\ln\left(\frac{A_2}{A_1}\right) - \ln\left(\frac{R_2}{R_1}\right)\right]$$

where T_1 and T_2 are the measured travel times of the wave of interest (first-arriving P-wave) to the near and far receivers respectively, A_1 and A_2 are the measured peak-to-peak amplitudes of the wave at the same receivers, and R_1 and R_2 are the distances to the receivers. For our experiment site, an average value for Q of 18.3 was determined from 21 different receiver pairs, with individual values ranging from 7.0 to 32.2.

To put the Q value determined for this site in context with other rock types, a compilation of Q values as a function of rock type was created from data contained in the literature. Most of the values were taken from Bradley and Fort (1966) and Vassilou and others (1984). The majority of these values were determined from laboratory conditions which will have some effect on the results. However, the scatter in the values is more a function of the wide variety of pressures, saturation levels, and frequencies used in the determination of the Q value rather than the method of determination. A plot containing the distributions of the Q values for different materials is shown in Figure 4. The data from our experiment are typical of values determined for unconsolidated sediments, although this category was under-represented in the data available. The alluvial material at our experiment site is more highly attenuating than most of the other rock types in this compilation.

Of course all this assumes a homogenous, isotropic media through which propagation occurs. In reality, however, the earth is neither homogenous nor isotropic. An example of this is shown in the following Figure 5, where waveforms gathered at a variety of locations are all plotted. In the first part of the figure, Figure 5A, the waveforms are scaled to each other, so one can see the relative magnitudes. The second half of the figure, Figure 5B, shows magnified versions of all the traces, so that the different seismic phases can be identified. (The different seismic phases will be discussed in more detail later.)

The top two traces are from sensors that are both approximately 50m from the source. It is clear that even though the distance between source and sensor is approximately the same for these two traces, the amplitudes in Fig 5B differ significantly. This difference could be caused by differences in the degree of coupling of sensors to the ground. However, care was taken to emplace the sensors in a similar fashion. A more likely explanation is that the path (which is N-S in direction) from the source to A11 has some heterogeneities (or a seismic region with greater attenuation) than the path from the source to A21 (which is in the S-W direction).

Seismic (geophysical) inhomogeneities or anisotropies affect more than just attenuation. In fact, the geophysical characteristics of a region can affect the amplitude, the arrival times, the modal composition, the velocity and the particle motion of a seismic signal. These are all important quanttities in seismic signal processing, and they can affect algorithm performance. The following discussion illustrates this, and the importance of knowing some geophysical characteristics of the area in which an unattended ground sensor system is deployed.

As mentioned earlier, the earth is neither a homogeneous nor isotropic seismic medium. However, over small regions, it is typical to model the ground by a layered earth model. In a layered earth model, each

layer is defined by the compression wave speed, the shear wave speed, the mass density and the layer thickness.

When seismic energy is incident on a layered medium, a variety of things can happen. As in Figure 2, when a compressional wave is obliquely incident on an interface, it can be transformed into 4 kinds of waves: a reflected compressional, a reflected shear, a refracted shear and a refracted compressional. Now, let's focus in on some more specific cases. When energy is obliquely incident (and at an angle greater than the critical angle ($\sin^{-1}(vo/v1)$), the downward traveling wave hits the interface and is totally reflected upward. At angles equal to or less than the critical angle, a large portion of energy is refracted into the medium below. At exactly the critical angle, the refracted wave travels horizontally along the boundary at the speed of the medium below. This is called a head wave. The travel time from source to a receiver will depend on the path. Also, in general, the signal at the receiver is a compilation of many waves, arriving at different times. The following figure is a theoretical plot of the travel times for various waves as a function of the source receiver separation. (Figure 6.)

Figure 7 is a similar plot using data from our experiment. You can see the effects of the different layering on arrival times for different separations. And it is also possible to see the different seismic phases superposed on each other when looking at the Figure 5b.

Clearly, the effects we have illustrated here (attenuation, anisotropy, modal composition, variation in travel time) can affect the quality and characteristics of seismic signals received by unattended ground sensors. In turn, these effects can affect the performance of the algorithms used to derive useful information from the seismic signals. For example, if time of arrival is being used for localization, the accuracy will depend on how well the differences in velocity structure are accounted for. Another example concerns attenuation. The performance of any detection algorithm will be affected by how much attenuation is being experienced between the sournce and sensor. This can also affect location algorithms based on signal amplitude. To make accurate conclusions, the attenuation or variation in attenuation must be considered. A final example concerns analysis that relies on particle motion. We have mentioned that in general a seismic signal is a compilation of different seismic phases arriving at different times. If an algorithm is relying on the particle motion of a certain phase to derive information, then the algorithm must have a way of guaranteeing that the portion of the wave it is working on is from the appropriate seismic phase.

In this paper we have presented a few physical phenomenon that can affect the performance of unattended ground sensor systems using seismic data. It is important that the UGS systems using seismic signal take these phenomenon into account, in either analysis, interpretation of results or both.

References:

1. Badri, M., and H. M. Mooney, 1987, *Q* measurements from compressional seismic waves in unconsolidated sediments, *Geophysics*, 52, 772-784.

2. Bradley, J. J., and A. N. Fort, Jr., 1966, Internal Friction in Rocks, in *Handbook of Physical Constants*, S. P. Clark, Jr., Ed., Geological Society of America Memoir 97, 175-193.

3. Dobrin, M. Introduction to Geophysical Prospecting. McGraw-Hill Book Company, New York, 1976.

4. Telford, W., L. Geldart, R. Sheriff and D. Keys. Applied Geophysics. Cambridge University Press, Cambridge, 1976.

5. Vassilou, M., C. A. Salvado, and B. R. Tittmann, 1984, Seismic Attenuation, in *CRC Handbook of Physical Properties of Rocks*, R. S. Carmichael, Ed., v 3, CRC Press, Inc., Boca Raton, Fl., 295-328.

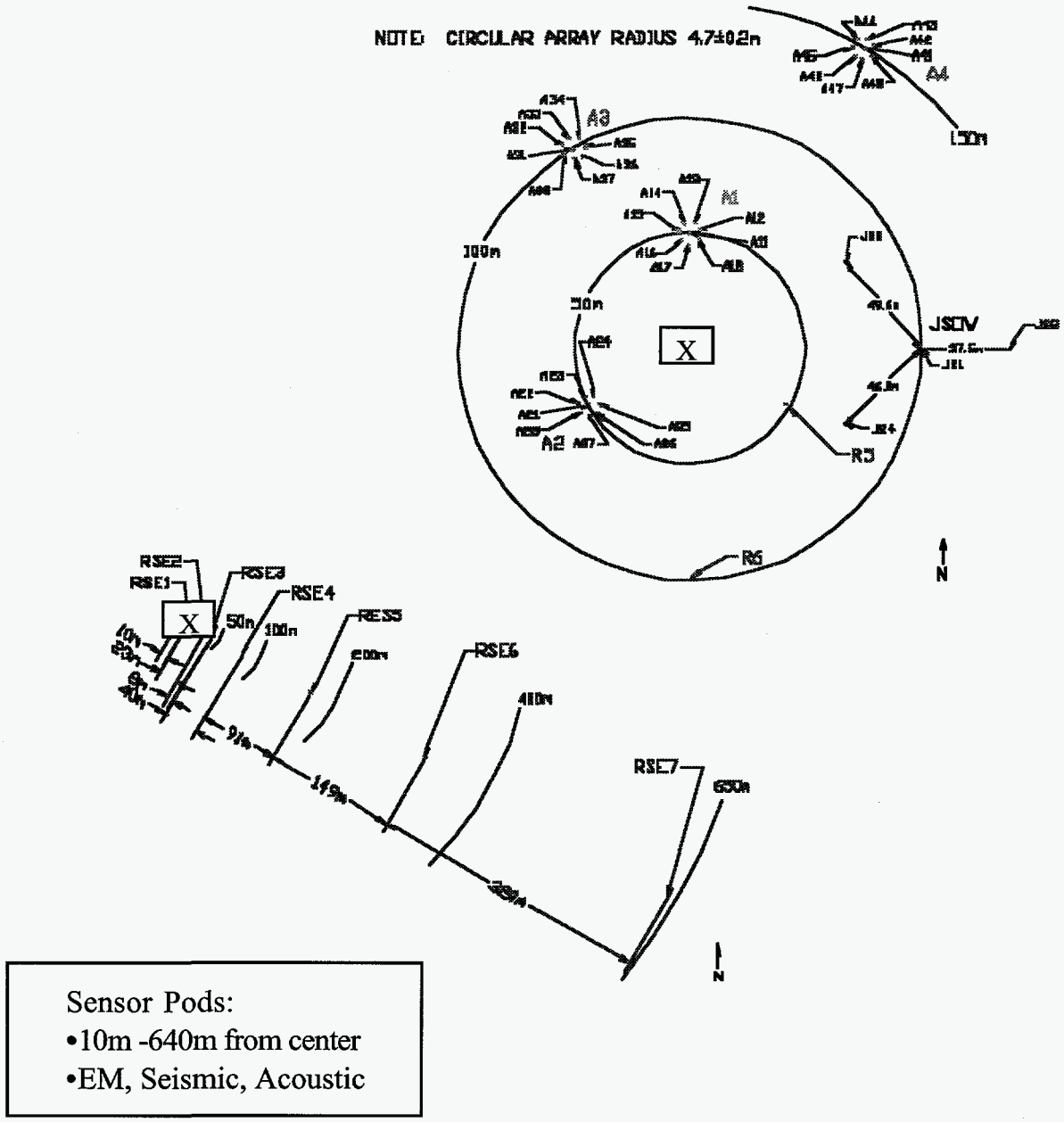

Figure 1: Unattended Ground Sensor Experiment at Nevada Test Site

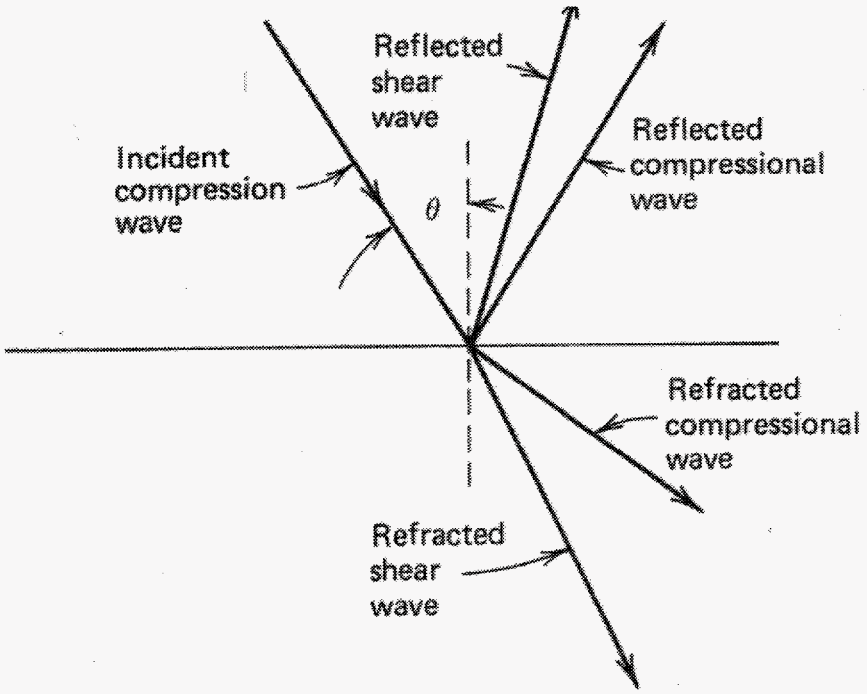

Figure 2: Waves resulting from a compression wave incident on a boundary. Waves are represented by rays. (After Dobrin[3].)

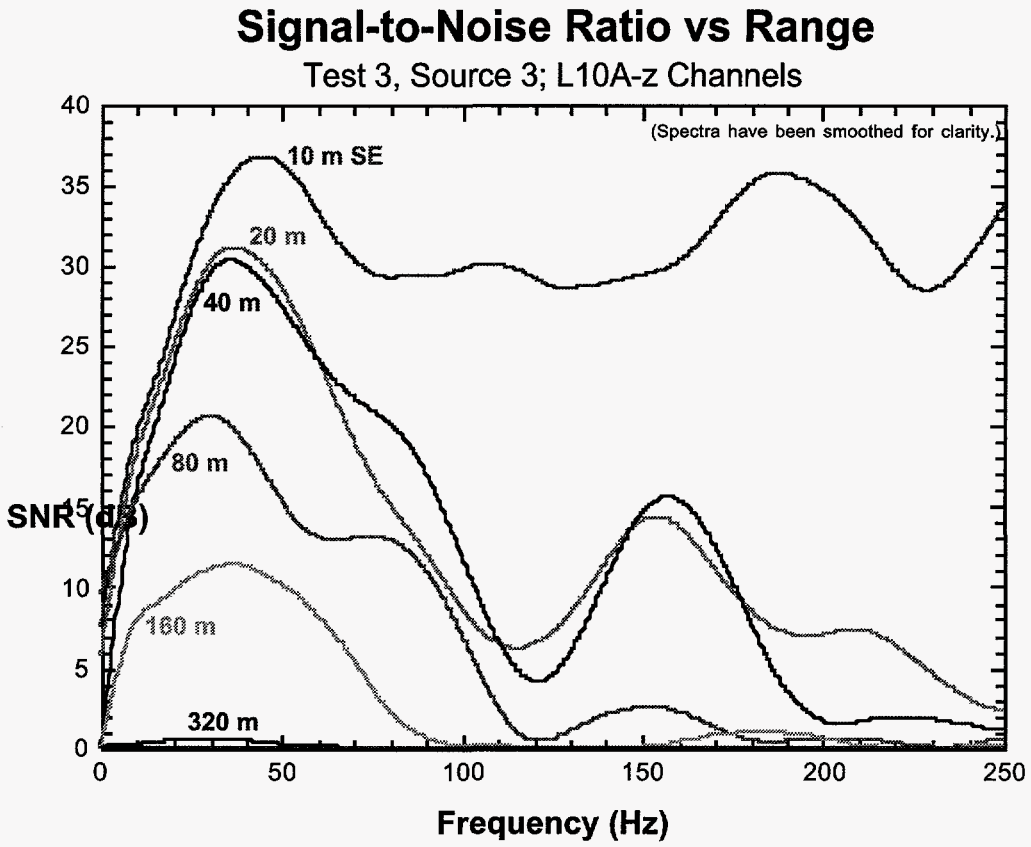

Figure 3: SNR vs. Frequency as a function of source-sensor distance.

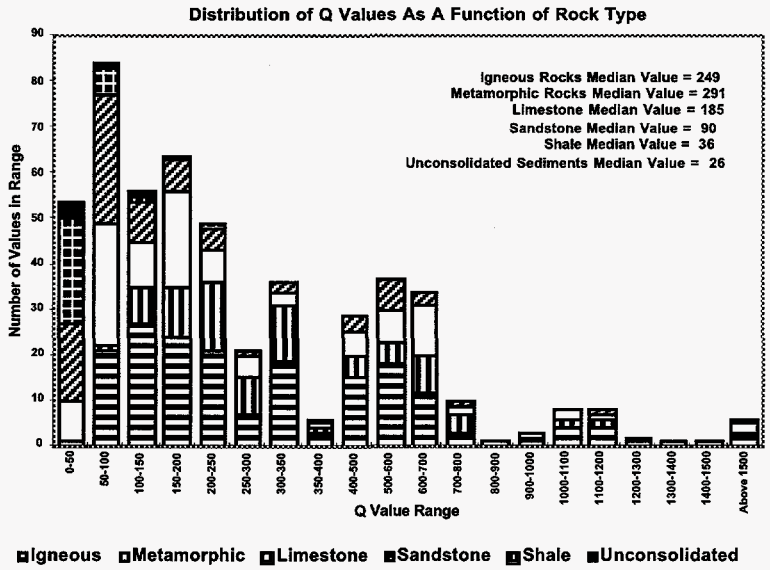

Figure 4: Composite histogram showing the distribution of the Q values as a function of rock type.

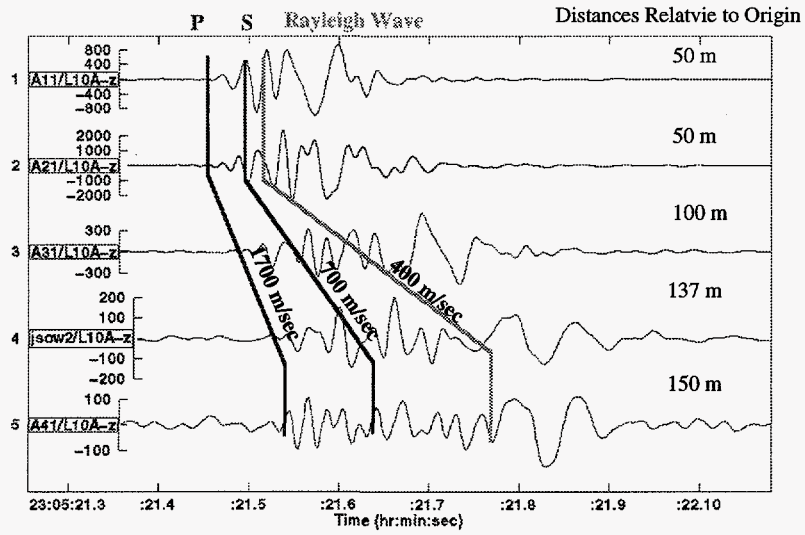

Figure 5A: Pseudo record section of the seismic recordings of the third hammer blow from Source 2 of Test 4. Each waveform has been filtered from 4 to 60 Hz. Each waveform's maximum amplitude has been scaled to the same size on the plots.

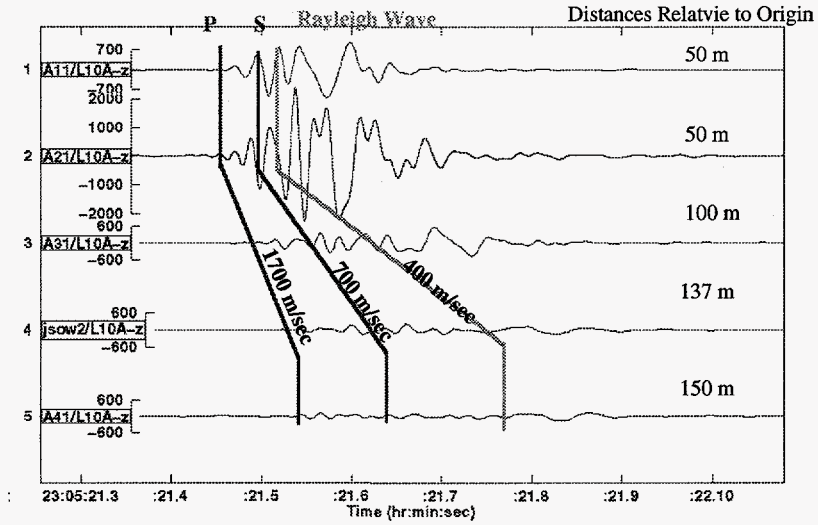

Figure 5B: Same pseudo record section as Figure 7.6.1-5 except the amplitudes are scaled relative to each other.

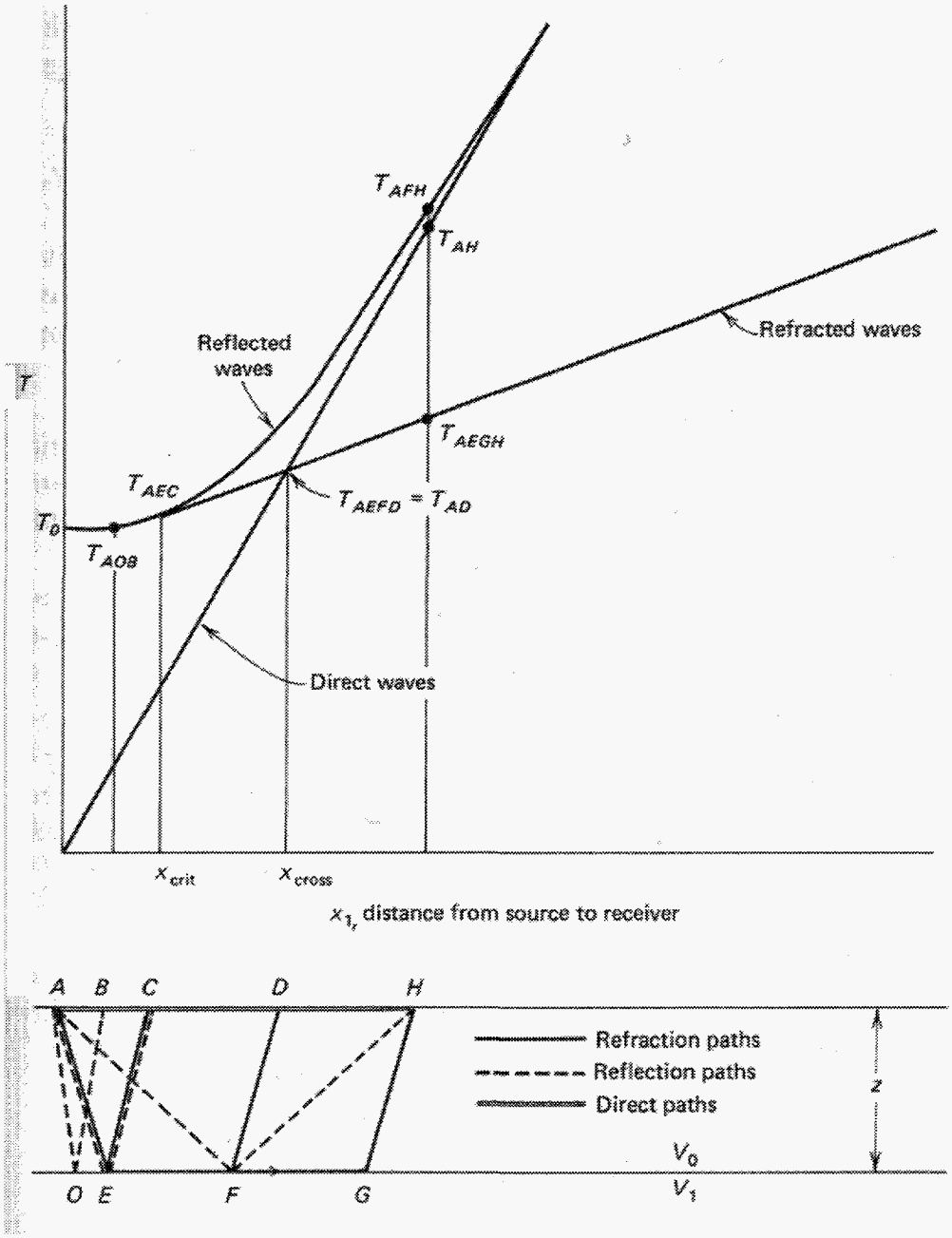

Figure 6: Theoretical relation between times of arrival for waves reflected and refracted from a horizontal interface. (After Dobrin[3].)

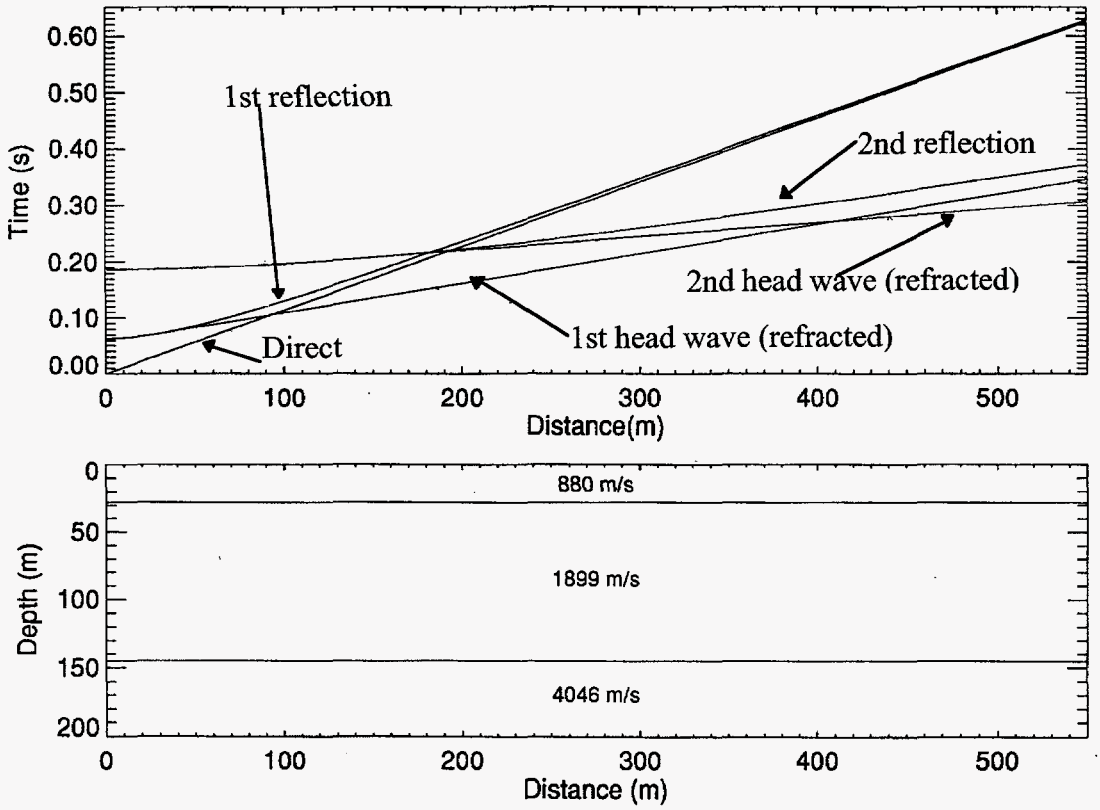

Figure 7: Actual arrival times for direct, reflected and refracted waves for the 3 layer model for our experiment.